



RESEARCH ARTICLE OPEN ACCESS

Genomic Loci for Sclerotinia Stem Rot Resistance and Chlorophyll Stability in *Brassica napus*: Integrating GWAS With Microbiome Insights

¹Department of Plant Breeding, Swedish University of Agricultural Sciences, Alnarp, Sweden | ²School of Integrative Plant Science, Cornell University, Ithaca, New York, USA | ³Centre of Estonian Rural Research and Knowledge, Jõgeva, Estonia | ⁴Lantmännen Lantbruk, Plant Breeding, Svalöv, Sweden

Correspondence: Kibrom B. Abreha (kibrom.abreha@slu.se)

Received: 30 April 2025 | Revised: 23 September 2025 | Accepted: 23 September 2025

Funding: This work was supported by grants from the Einar and Inga Nilssons Foundation for Surgical Research and Research in Agriculture. RRV is supported by the SLU Centre for Biological Control.

Keywords: chlorophyll index | genomic regions | lesion length | rapeseed | relative lesion area | Sclerotinia sclerotiorum

ABSTRACT

Sclerotinia Stem Rot (SSR) disease is one of the most serious diseases affecting the yield and quality of oilseed rape (*Brassica napus*). Understanding the genetic basis of the resistance trait in oilseed rape to SSR and microbiome composition for enhanced resistance is crucial for developing resistant varieties and sustainably mitigating the impact of the disease. In this study, in a panel of 168 oilseed rape accessions, the most resistant (NGB 13503 and NGB 13834) and susceptible (NGB 13497 and NGB 13897) accessions are identified. A Genome-wide association study (GWAS) identified 47 SNPs linked to the SSR lesion length, lesion area, and lesion relative to the leaf area. Among the SNPs significantly linked to lesion length were Bn-A04-p10555408, Bn-A07-p12487549, Bn-A09-p4652268, Bn-A09-p4916858 and, to our knowledge, these SNPs have not been previously linked to SSR resistance in oilseed rape. Moreover, the study identified 24 SNPs linked with chlorophyll content before SSR inoculation (SPADH), after the SSR inoculation (SPADI), and chlorophyll index (CI). Maintaining the chlorophyll level is correlated with SSR resistance. Furthermore, bacterial taxa (e.g., *Pseudomonas, Methylobacterium*, and *Aquabacterium*) and fungal taxa (e.g., *Mycosphaerellales, Thelebolales*, and *Akanthomyces*) were enriched in the resistant compared to the susceptible oilseed rape accessions. The SNPs linked to lesion length showed consistent haplotype variation between these selected accessions. Given the absence of complete resistance against SSR, the study provides insights into the significance of maintaining chlorophyll levels and considering microbiome composition for enhancing the level of existing partial resistance to SSR in oilseed rape.

1 | Introduction

Oilseed rape (*Brassica napus* L.), formed by natural interspecies hybridization of *Brassica rapa* (AA; 2n = 20) and *B. oleracea* (CC; 2n = 18), is an economically important allotetraploid (AACC; $2n = 4 \times = 38$) oilseed crop. Currently, oilseed rape is cultivated

globally, providing an estimated annual production exceeding 75 million tons (FAOSTAT 2023). It is one of the most widely used vegetative oils along with soybeans and palm oil. The crop has high seed protein content and high seed oil yield and quality, which is rich in mono and polyunsaturated fatty acids and tocopherols (Stepien et al. 2017; Rout et al. 2018; Chew 2020). As

This is an open access article under the terms of the Creative Commons Attribution License, which permits use, distribution and reproduction in any medium, provided the original work is properly cited.

© 2025 The Author(s). Plant-Environment Interactions published by New Phytologist Foundation and John Wiley & Sons Ltd.

a result, oilseed rape is used as food, a protein-rich feed for animals, and has multiple industrial applications (Raboanatahiry et al. 2021).

The small number of founder parents involved in allopolyploidization events in oilseed rape, strong breeding selection for high seed oil quality, and intensified cultivation for higher yield have limited the oilseed rape genetic pool (Wu et al. 2014; Liu et al. 2022). This has contributed to various fungal diseases causing serious losses in oilseed rape yield and quality (Van de Wouw et al. 2016). Particularly, the fungal pathogen Sclerotinia sclerotiorum, the causal agent of the devastating Sclerotinia Stem Rot (SSR) disease, is present in all major oilseed rape growing areas and is causing significant yield and quality losses in oilseed rape (Derbyshire and Denton-Giles 2016; Neik et al. 2017). SSR has a broad host range, including several Brassica oilseed crops (Ficke et al. 2018), indicating its significant importance in oilseed production in general. Up to 80% yield loss due to SSR disease has been reported in major oilseed rape growing areas (Wu et al. 2016). The emergence of virulent and fungicide-resistant strains of the pathogen could lead to frequent outbreaks in oilseed rape growing areas (Derbyshire and Denton-Giles 2016). Therefore, there is a pressing need to develop effective and sustainable methods to reduce SSR disease pressure and consequently minimize seed yield and quality losses.

Enhancing the oilseed rape resistance against SSR disease through genetic improvement is the most environmentally sustainable approach for managing SSR. Identifying resistance genotypes with complete resistance against SSR in diverse oilseed rape germplasm is essential for developing resistant varieties. Despite considerable breeding efforts, however, oilseed rape varieties with complete resistance against SSR have not been developed so far (Neik et al. 2017; Ding et al. 2021). This is partly attributed to the aggressiveness of the pathogen employing diverse strategies to overcome the host resistance and limited understanding of the oilseed rape–SSR pathosystem and genetic regulation of the host resistance.

Multigenic resistance governed by quantitative trait loci (QTLs) is the most important form of oilseed rape resistance against SSR (Wu et al. 2016; Neik et al. 2017). Nevertheless, only a few QTLs related to SSR resistance have been identified so far, mainly using bi-parental mapping populations of the crop (Derbyshire and Denton-Giles 2016; Wu et al. 2016). Bi-parental population-based QTL mapping is only restricted to the diversity and recombination events between a few founder genotypes, thus resulting in low resolution of the genetic map (Dahanayaka and Martin 2023). Consequently, the QTLs identified so far have limited application for improving the SSR resistance in oilseed rape.

Genome-wide association study (GWAS), which takes advantage of the phenotypic variation and historical recombination in natural populations, is a powerful tool to identify quantitative trait loci (QTLs) linked to important traits of interest (Korte and Farlow 2013). GWAS uses thousands of SNPs generated through next-generation sequencing technologies, and it is instrumental for establishing marker-trait association (MTA) and the development and validation of genetic markers for use in marker-assisted selection (MAS). Indeed, GWAS has been successfully used to identify QTLs linked to disease resistance (Wu

et al. 2016; Roy et al. 2021), as well as other important agronomic traits such as yield and oil quality-related traits in oilseed rape (Zhao et al. 2022; Xiang et al. 2023).

Host resistance is a result of the host, pathogen, and environment interactions involving biotic and abiotic factors. Pathogen infection significantly reduces the photosynthetic performance and subsequently the yield and quality. Maintaining the photosynthetic capacity could be one mechanism of SSR resistance in oilseed rape, as recently shown, the possible involvement of photosynthesis in silicon (Si) induced resistance against the pathogen (Feng et al. 2021). Chlorophyll levels could be used as a proximal trait to measure disease in crops (Odilbekov et al. 2018; Koc et al. 2022). Moreover, with the advent of sequencing technologies and analysis tools, there is growing evidence regarding the role of microbes affecting host-pathogen interactions (Rybakova et al. 2017; Liu et al. 2021). Since no complete resistance to SSR has been identified in diverse germplasm screening or developed through breeding, understanding the genetic basis for maintaining the photosynthesis level and microbiome composition would be invaluable for enhancing and developing effective disease management strategies.

In the present study, we have identified oilseed rape genotypes with partial resistance against SSR and identified marker-trait associations (MTAs) for the SSR resistance and chlorophyll levels during the SSR infection. Furthermore, using the most relatively resistant and susceptible genotypes, we showed differential microbiome composition in these genotypes and established the correlation to the SSR resistance MTAs identified using GWAS.

2 | Materials and Methods

2.1 | Plant Material and Experimental Setup

A panel of 168 oilseed rape accessions, obtained from the Nordic Genetic Resource Centre (NordGen), consisting mostly of varieties from Nordic origin, was used for a Genome-wide analysis study (GWAS) analysis to identify genomic regions linked to SRR resistance (Table S1). Ten plants from each accession were grown in seedling trays, and at 3 weeks, leaves from every plant were collected from each accession for genotyping using the Brassica 19K Illumina SNP array. Three seedlings per accession were each transferred into 2L potting soil separately and arranged in a completely randomized (CRD) design with three replications in a controlled climate chamber facility with adjustable climate conditions at the Swedish University of Agricultural Sciences at Alnarp. The plants were grown in the chamber under long-day conditions (16/8 h photoperiod, 25°C/20°C Day/ night, and 65% RH) until evaluated for resistance against SSR using detached leaf assays.

2.2 | Fungal Strain Maintenance and SSR Resistance Evaluation

S. sclerotiorum isolate was obtained from Lantmännen and aseptically maintained on potato dextrose agar (PDA) at 4° C in the dark. A 5 mm plug was placed in the middle of freshly prepared

PDA plates and incubated at room temperature in the dark. Agar plugs (3 mm Ø) were punched from the actively growing edge of 3-day-old fungal PDA plates. For detached leaf assays, three leaves per accession per plant were excised from the 6-week-old plants, placed in a transparent plastic box (39×29×12.5 cm), and humidified to 100% with a water-soaked gauge to maintain higher humidity. The gauge was separated from the leaves by a plastic net. One fungal plug (3 mm Ø) was placed on both sides of the midrib on the abaxial surface of the detached leaves. Boxes with inoculated detached leaves were sealed with parafilm and incubated at room temperature and a 16:8 photoperiod. Lesion diameter and leaf pictures were taken at 3 days post inoculation (3 dpi).

2.3 | Phenotyping and Data Analysis

The diameter of the lesion area (lesion length, LL) on the detached leaves was measured manually at 3 days post inoculation (dpi). Immediately, pictures of each leaf were taken using a mounted NIKON D3500 (Nikon, Tokyo), and the pictures were investigated on a leaf basis to measure the lesion area (LA) and calculate the relative lesion area (RLA), which is the area of the lesion relative to the area of the leaf (RLA=lesion area/total area of the leaf), using ImageJ. According to this measurement, the 10 most relatively resistant and 10 most susceptible accessions to SSR were selected for microbiome recruitment analysis (details below).

Leaf chlorophyll concentration before infection (SPADH) was measured immediately after the leaves were detached and placed in the transparent infection boxes. Leaf chlorophyll concentration was also measured at 3 dpi after infection (SPADI). Both SPADH and SPADI were measured with the MC-100 chlorophyll meter (Apogee Instruments Inc., Logan) at five locations of each leaf, and average data was expressed as SPAD values. The chlorophyll index (CI) was calculated in terms of chlorophyll loss under infection conditions by employing the following formulae.

 $CI = \frac{Chlorophyll \ content \ at \ 3 \ days \ after \ inoculation}{Chlorophyll \ content \ before \ inoculation} \times 100 \ (\%)$

2.4 | SNP Array Genotyping of Oilseed Rape Accessions

One leaf from each of the 10 plants from each accession was collected, piled, and punched with a 3 mm cork. The 3 mm discs of each accession were placed in 96-well plates provided as part of the BioArk Leaf collection kit from LGC Biosearch Technologies (Berlin, Germany). During sampling, the well plates were placed on ice to slow down the physiological process and drying of the excised discs. Upon collecting the leaves from all accessions, the plates were covered with cotton, freeze-dried for 3 days, and sent to the sequencing company (LGC Genomics GmbH, Germany). The genotyping was done using the Brassica 19K Illumina SNP array (Illumina Inc., San Diego, CA). A total of 18,579 informative single-nucleotide polymorphism (SNP) markers, representing both the *B. rapa* A-genome and *B. oleracea* C-genome, were obtained. Of these, 14,266 SNPs were mapped to the *B. napus* reference genome (Darmor-bzh), and marker distribution across

the genome was visualized using the Scientific and Research plot tool (SRPlot) (Tang et al. 2023). A total of 12,738 high-quality (missing data < 10%, MAF > 0.05) SNPs were filtered in TASSEL v.5.2.86 (Bradbury et al. 2007), and used for further analysis.

2.5 | Linkage Disequilibrium (LD) and Population Structure

Using the 12,738 high-quality SNPs, the pairwise LD values (r^2) , which refer to the nonrandom association of alleles at different loci, were calculated (window size=50 markers) in TASSEL v.5.2.86 (Bradbury et al. 2007). The LD (r^2) values were plotted against the genetic distance (bp) between marker pairs for each chromosome using the LD score plotting script in R Studio as described previously (Remington et al. 2001). The pattern of genome-wide LD decay was considered at the r^2 =0.1 threshold, which is at half compared to the maximum LD (r^2) value.

2.6 | Genome-Wide Association Study (GWAS)

Best linear unbiased predictions (BLUPs) for the measured traits from the 168 oilseed rape accessions were estimated using the Multi Environment Trial Analysis with R (META-R) (Alvarado et al. 2020), and were used as a phenotype, and their corresponding genotyping data was used for the GWAS analysis. The GWAS analysis was performed with the most robust models, bayesian-information and linkage-disequilibrium iteratively nested keyway (BLINK) (Huang et al. 2018) and fixed and random model circulating probability unification (FarmCPU) (Liu et al. 2016) with GAPIT Version 3 in RStudio (Wang and Zhang 2021). The relative kinship matrix (K) was computed with the VanRaden method (VanRaden 2008); population structure was visualized with a heatmap performed in GAPIT in R (Wang and Zhang 2021). The suitability of the models BLUPs for the GWAS analysis was assessed using histograms, quantilequantile (Q-Q) plots, and scatter plots. SNPs with FDR-adjusted p < 0.001 [$-\log_{10}(p) > 3$] were considered significantly associated with the phenotypic traits measured.

2.7 | Effect of the Significant SNPs on the Phenotypes Measured

All the oilseed rape accessions were grouped according to the allele variation at the most significant SNPs associated with the traits measured. To determine the significance among groups formed based on favorable and alternative alleles, a two-sample *t*-test was conducted in R statistical software v.4.4.1.

2.8 | Microbiome Recruitment in Relatively Resistant and Susceptible Accessions of Oilseed Rape

2.8.1 | DNA Extraction, Amplification, and Sequencing

DNA was extracted from the collected leaf samples of the most relatively resistant and susceptible accessions using a modified DNeasy PowerSoil Pro kit (Qiagen, CA, USA) protocol, as

Plant-Environment Interactions, 2025 3 of 18

mentioned below, with three replications per accession. The frozen leaf samples were ground to a powder in a pre-chilled mortar and pestle filled with liquid nitrogen before proceeding with the manufacturer's recommended protocol. The wash step with solution EA was repeated three times to ensure the removal of phenolic compounds. The extracted DNA's quality and quantity were evaluated using a Nanodrop (Nanodrop 8000 Thermo Fisher Scientific, USA).

For bacteria, the V5-V6 regions of the bacterial 16S rRNA gene were amplified using the primer pair 799F (AACMGGATTAGATACCCKG) and 1115R (AGGGTT GCGCTCGTTRC). For fungi, the internal transcribed spacer 1 (ITS1) region was targeted by the primer pair ITS1Kyo2F (TAGAGGAAGTAAAAGTCGTAA) and ITS86R (TTCAAAGATTCGATGATTCA). For each sample, PCR reactions were performed using a 20 µL mixture comprising 1× MyTaq buffer containing 1.5 units of MyTaq DNA polymerase (Bioline GmbH, Luckenwalde, Germany), 2 µL of BioStabII PCR Enhancer (Sigma-Aldrich Co.), ~1-10ng of template DNA, and 15 pmol of the respective forward and reverse primers, as mentioned above. PCR was carried out using the following program: predenaturation at 96°C for 1 min, denaturation at 96°C for 15s, annealing at 55°C for 30s, and extension at 70°C for 90s, followed by 30-33 cycles of amplification of prokaryotic genes and 35-40 cycles of amplification of eukaryotic genes. The amplified PCR products were purified with Agencourt AMPure beads (Beckman Coulter, Brea, CA, United States). Illumina libraries were constructed using the Ovation Rapid DR Multiplex System 1-96 (NuGEN Technologies Inc., California, USA) with 100 ng of purified amplicon pool DNA for each type. After library construction, the Illumina libraries (Illumina Inc., CA, USA) were combined and subjected to size selection through preparative gel electrophoresis. Sequencing was performed on an Illumina MiSeq platform at the LGC's sequencing facility in Berlin (LGC Genomics GmbH, Germany).

2.8.2 | Amplicon Data Processing and Analysis

After sequencing, primers, and adapters were removed from amplicon data using cutadapt v4.7 (Walker et al. 2014), and the quality of the reads was improved with the same tool. Next, high-quality filtered amplicon reads were demultiplexed with QIIME2 v2022.8 (Bolyen et al. 2019), and the DADA2 plugin (Callahan et al. 2016) of QIIME2 was employed to denoise, dereplicate, and remove chimeric reads. The resulting amplicon sequence variants (ASVs) were taxonomically classified using the pre-trained 16S rRNA database SILVA v138.1 (Quast et al. 2013) and the ITS database UNITE v9 (Nilsson et al. 2019). A Naive Bayes classifier was used to train databases. ASVs were unassigned, and ASVs assigned to chloroplasts and mitochondria were removed.

2.9 | Statistical Analysis

R v4.2.0 (Team R Core 2013) was used for all the statistical analyses. A phyloseq object comprising ASVs table, taxonomy, sequence, and sample metadata file was made using the R package "phyloseq v1.26.1" (McMurdie and Holmes 2013). Before statistical analysis, the phyloseq object was rarefied. The plot_taxa_composition() function of the "microbiome v3.19" (Leo

Lahti 2017) and "microbiomeutilities v0.99" (Lahti 2018) packages were used to plot the relative abundance (%) of taxons. Data normality was checked with the Shapiro.test() function from the "stats v3.6.2" (R Core Team 1970) package. Alpha diversity metrics "Chao1" and "Shannon" were computed with "vegan v2.5.1" (Dixon 2003), and the same package Wilcoxon rank sum test was performed to check the difference in the sample groups. Linear discriminatory analysis (LDA) was performed with "microbiomeMarker v1.2.1" package (Cao et al. 2022); cut-off value for LDA was set at 2 and p-value at <0.05.

2.10 | Data Availability

All the amplicon data (16S and ITS) were submitted to the sequence read archive repository under BioProject: Id PRJNA1063738.

3 | Results

3.1 | Phenotypic Variability Within the Oilseed GWAS Panel

A GWAS panel composed of 168 diverse oilseed rape accessions was evaluated for Sclerotinia stem rot (SSR) lesion length (LL), lesion area (LA), and relative lesion area (RLA). Leaf chlorophyll concentration was measured before inoculation (SPADH) and after inoculation (SPADI) with SSR, respectively, and the chlorophyll index (CI) in these accessions was calculated using these measurements. The summary statistics, such as mean, range, and coefficient of variance for the traits measured, are presented in Table 1.

The mean LL was $58.5\pm1.56\,\mathrm{mm}$ with the shortest $53.5\,\mathrm{mm}$ and the longest $63.9\,\mathrm{mm}$, whereas LA ranged from 17.7 to $22.6\,\mathrm{cm}^2$ with a mean value of $19.5\pm0.6\,\mathrm{cm}^2$. On average, the lesion covered 48% of the inoculated leaf area (RLA). The CV was higher for LA (56%) and RLA (52%) compared to LL (29%), highlighting the importance of measuring various aspects of the lesion growth and leaf to understand the growth of the disease on inoculated

 $\textbf{TABLE 1} \quad | \quad \text{Mean and coefficient of variation for the measured traits.}$

Trait measured	Mean ± SD	Range	CV (%)
Lesion length (LL) (mm)	58.45 ± 1.56	53.53-63.87	29
Lesion area (LA) (cm²)	19.46 ± 0.55	17.66-22.61	56
Relative lesion area (RLA) (%)	48 ± 0.02	45–57	52
Chlorophyll (healthy)—SPADH	37.21 ± 0.94	34.63-40.11	9
Chlorophyll (inoculated)— SPADI	18.86 ± 0.91	15.25–22.06	24
Chlorophyll index (CI) (%)	50.36 ± 1.98	41.47–56.65	21

leaves. We found a strong positive correlation ($r^2 = 0.60$) between LL and LA (Figure 1); however, RLA showed a weak correlation to these SSR resistance traits (Figure 1).

Although there was no correlation (Figure 2), the RLA reflects the dropping of the chlorophyll content due to the infection from 37.21 in SPADH to 18.86 in SPADI. CI value ranges from 41.47% to 56.65% (Table 1), and it is significantly correlated to SPADI (r^2 =0.94) while SPADH has little effect (r^2 =0.20) (Figure 1). The CV for SPAD increased from 9% in SPADH to 24% in SPADI, indicating the chlorophyll content in the accessions was affected differently by the SSR inoculation.

3.2 | SNPs Distribution, LD Decay, and Population Structure

The high-quality 12,738 SNPs distributed throughout the Agenome (7713) and C-genome (5025) were visualized with SRPlot. A non-uniform pattern of SNPs distribution per 1

million base window was observed across the 19 chromosomes, with the most SNPs mapped on chromosome A03 (1282) and the least on chromosome C01 (536).

The LD squared correlation coefficient (r^2), for all the 1237 high-quality SNP markers, was used for estimating the extent of LD decay. Genome-wide LD decayed to r^2 =half decay at 0.53 Mb (Figure 2B). The LD decay varied between 0.39 Mb for A- and 1.07 Mb for C-subgenomes as well as across the chromosomes, with the longest 4.83 Mb for C01 and the shortest 0.25 Mb for A07 (Table 2). Based on this LD decay, all significant SNPs within LD decay distance values in each chromosome were considered as part of the same QTL.

A clustering heat map created using a kinship matrix and principal components analysis structured the 168 accessions into two subpopulations (Figure 2C,D). In both analyses, the accessions were mostly grouped according to their growth habit, winter accessions or spring accessions. PC1 and PC2 explain 34.5% and 4% of the total variation, respectively (Figure 2D). The grouping in

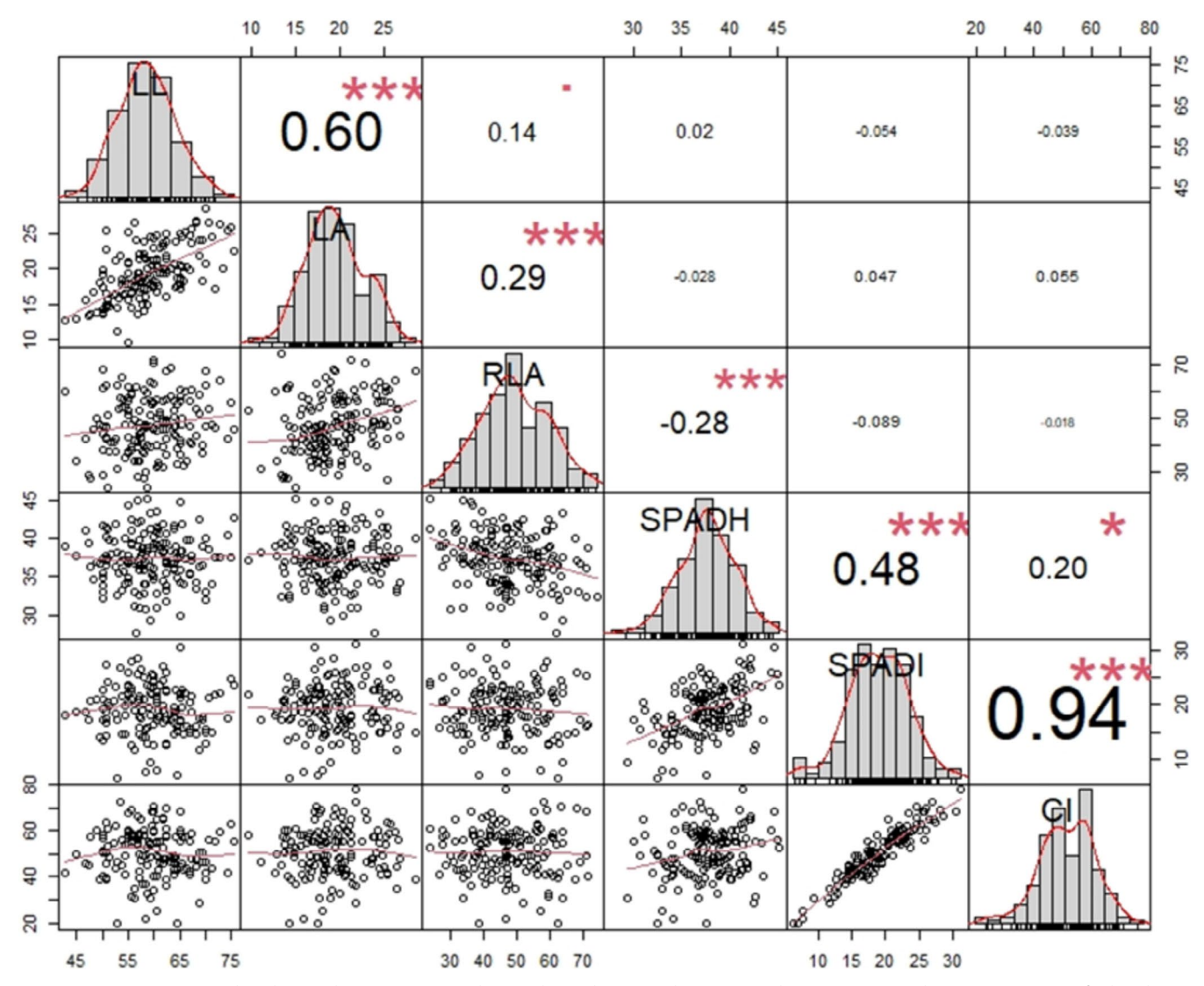


FIGURE 1 | Frequency distribution, bivariate scatter plots, and correlation analysis among the traits measured in 168 accessions of oilseed rape. Sclerotinia stem rot (SSR) lesion length (LL), lesion area (LA), and the relative leaf area (RLA) measured at 3 days post inoculation (dpi). Leaf chlorophyll concentration was measured before inoculation (SPADH) and at 3 dpi (SPADI) with SSR, respectively, and the chlorophyll index (CI) was calculated from both measurements. Significance level of the correlation values: ***p < 0.001, **p < 0.05, p < 0.1.

Plant-Environment Interactions, 2025 5 of 18

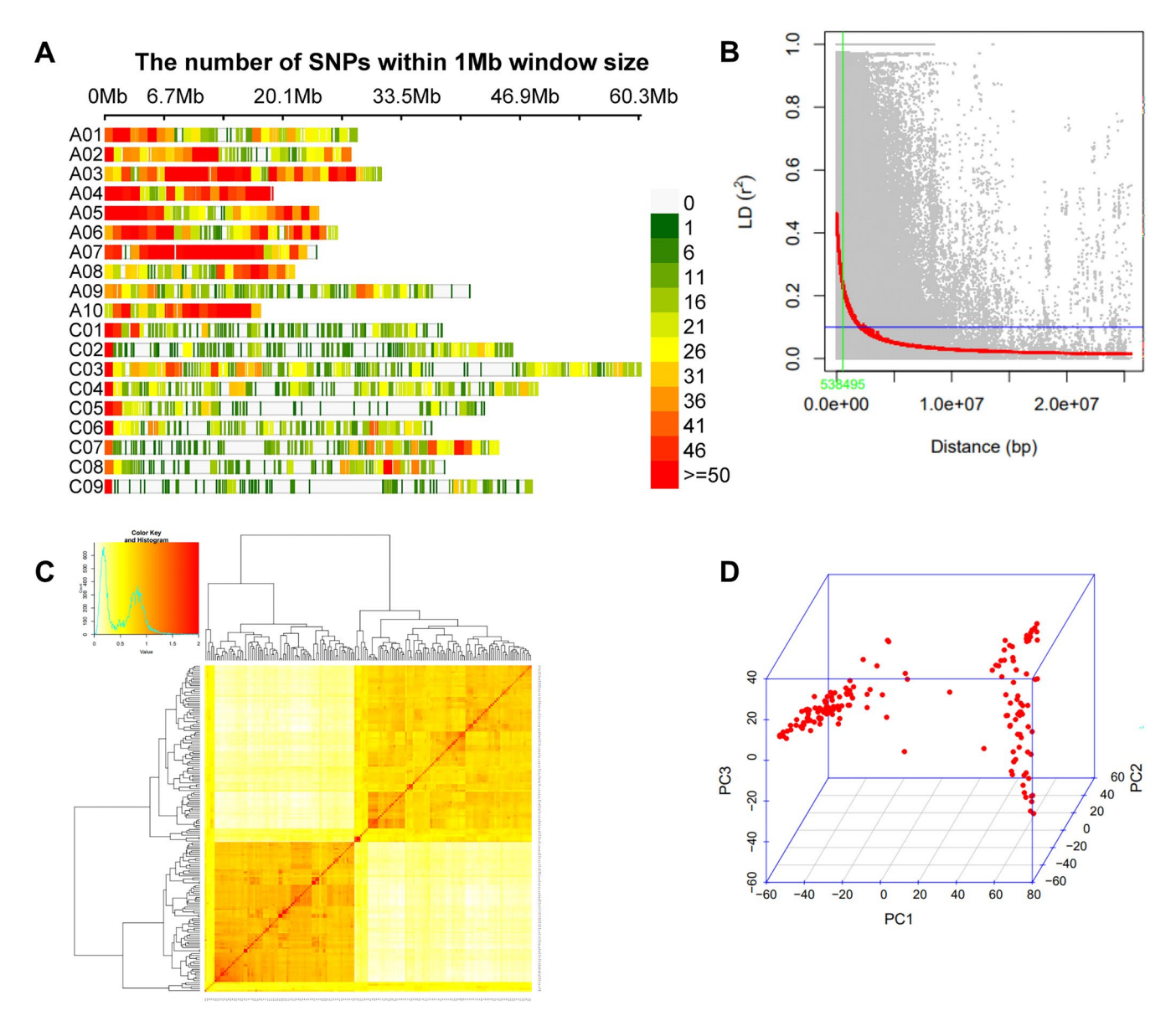


FIGURE 2 | (A) Number of SNPs within a 1 Mb window size of *Brassica napus* genome; (B) LD decay scatter plot with r^2 values of pairwise SNPs; (C) Kinship plot as a heatmap of the VanRaden kinship matrix; (D) Principal components analysis (PCA).

principal components analysis corresponds with the VanRaden kinship matrix clustering.

3.3 | Genome-Wide Marker-Trait Associations

The main objective of this study was to identify SNPs significantly related to SSR resistance traits and chlorophyll stability in the oilseed rape accessions. The normal distribution of the histograms (Figure 1) indicated the suitability of the traits' BLUPs for GWAS analysis. For the six traits measured, a total of 71 significant MTAs, 34 in A and 37 in C sub-genomes, were detected with the FarmCPU and BLINK models (*p*-value <0.001). Except for 10 MTAs associated with the chlorophyll index, all the MTAs associated with the other traits were detected in both GAPIT models. The MTAs were distributed across the 10 chromosomes of the A subgenome and seven chromosomes of the C subgenome, except for chromosomes C01 and C09. The highest number of MTAs was located on Chr-C02 (17 MTAs) followed by

chromosome A01 (11 MTAs). The MTAs detected on C02 were associated with the chlorophyll index, chlorophyll after infection (SPADI), and lesion length. Some MTAs on chromosome A01 and C02 were also associated with the relative lesion area (RLA). Except for LA, all the traits had MTAs from subgenomes A and C.

3.4 | MTAs for Sclerotinia Stem Rot (SSR) Resistance Traits in Oilseed Rape

A total of 47 MTAs on 12 chromosomes, six from each subgenome, were found significantly (p < 0.001; $-\log_{10}(p) > 3$) associated with the Sclerotinia stem rot (SSR) resistance traits lesion length (LL), lesion area (LA), and the relative lesion area (RLA) (Table 3, Figure 3). Among the 10 MTAs linked with the LL were two on chromosome C04 and two on C08, as well as two MTAs, Bn-A09-p4652268 and Bn-A09-p4916858, on chromosome A09.

6 of 18 Plant-Environment Interactions, 2025

TABLE 2 | Linkage disequilibrium for the chromosomes in subgenome A and subgenome C of oilseed rape.

	LD decay		
Chr	(Mb)	Chr	LD decay (Mb)
A01	0.21	C01	4.83
A02	2.03	C02	3.74
A03	0.21	C03	1.33
A04	0.28	C04	0.72
A05	0.5	C05	0.32
A06	0.3	C06	1.15
A07	0.25	C07	0.49
A08	0.8	C08	0.63
A09	0.87	C09	1.64
A10	0.41		
Subgenome A	0.39		
Subgenome C	1.07		
Whole genome	0.53		

For the LA, nine MTAs were found in the A sub-genome across five chromosomes (A01, A02, A03, A04, and A06), and 17 MTAs were in the C sub-genome distributed across four chromosomes (C02, C03, C04, and C07). Based on an average LD decay of 0.53 Mb, 13 MTAs linked to the SSR-IA were classified into four QTLs, with three MTAs on chromosome A04 (48.49-51.37 Mb), two MTAs on C02 (25.69-25.72 Mb), three MTAs on C04 (32.45-32.85 Mb), and five MTAs on C07 (31-31.13 Mb) (Table 3). Other MTAs associated with LA were Bn-A01-p2291940 (2.29 Mb), Bn-A01-p24575577 (24.58 Mb), and Bn-A01-p4353657 (4.35 Mb) on chromosome A01 (Table 5). All the MTAs associated with the RLA were located in the A subgenome. Among the three MTAs were Bn-A01-p5265598 (5.26 Mb) and Bn-A01-p5269368 (5.26 Mb) (Table 3). Similarly, four MTAs found at 14.76Mb (Bn-A07-p14766907 and Bn-A07-p14768265), 14.77 Mb (Bn-A07-p14770619), and 14.79 Mb (Bn-A07-p14792267) could be considered one QTL.

3.5 | MTAs for Chlorophyll Content in SSR-Infected Oilseed Rape

The GWAS analysis identified 24 MTAs significantly linked to the chlorophyll traits; seven for SPAD before inoculation (SPADH), six for SPAD at 3 days post inoculation (SPADI), and 11 MTAs for chlorophyll index (CI) (Table 4, Figure 4). All the MTAs for SPADH and six for SPADI were identified in both FarmCPU and Blink models, while for CI six MTAs were identified in the FarmCPU and four were identified in the Blink model. SNP markers Bn-scaff_20461_1-p249973 and Bn-scaff_20461_1-p178421 located on chromosome C02 and Bn-scaff_16361_1-p1343410 located on chromosome C08 were closely linked to CI and SPADI (Table 4).

Six of the seven MTAs linked to the SPADH were identified in subgenome A, including two MTAs located on chromosome A06,

while there was only one MTA that was located on C06. Conversely, four of the six MTAs significantly associated with SPADI were identified in the C subgenome: Bn-scaff_20461_1-p249973 (9.42 Mb) and Bn-scaff_20942_1-p1093417 (10.93 Mb), as well as Bn-scaff_20461_1-p178421 (0.18 Mb) and Bn-scaff_15712_5-p313157 (0.31 Mb) on chromosome C02 (Table 4).

For CI, four MTAs were on chromosome C02, three on C02, and one on each subgenome A chromosomes A02, A04, and A05. Three of the four MTAs identified on C02 were located on 9.42 Mb (Bn-scaff_20461_1-p249973), 9.55 Mb (Bn-scaff_20461_1-p110039), and 9.56 Mb (Bn-scaff_20461_1-p99520) (Table 5). The three are within the LD region for chromosome C02, indicating the presence of a QTL region on this chromosome. Likewise, the three MTAs for CI identified on C08 are at 28.81 Mb (Bn-scaff_16361_1-p1343410), 28.41 Mb (Bn-scaff_16361_1-p935272), and 33.36 Mb (Bn-scaff_16197_1-p659483) (Table 4). These SNPs within the LD score indicate they are linked.

3.6 | Phyllosphere Microbiota Diversity of Rapeseed in Resistance and Susceptible Accessions

This study used 16S rRNA gene sequencing to elucidate the diversity and composition of microbial (bacterial and fungal) communities within the phyllosphere of resistant and susceptible rapeseed varieties and to understand their potential role in plant resistance mechanisms.

3.6.1 | Bacterial Communities

Our analysis revealed significant differences in the bacterial alpha diversity between the resistant and susceptible rapeseed varieties (Figure 5A). The bacterial richness, as indicated by the Chaol estimator, was significantly higher in susceptible varieties (Wilcoxon test, p-value <0.005). Additionally, the Shannon index, which accounts for both richness and evenness, also showed significantly higher overall diversity in the susceptible varieties (Wilcoxon test, p-value <0.005). These results suggest that the phyllosphere of susceptible rapeseed varieties harbors more diverse communities. In contrast, the fungal microbiota diversity did not exhibit significant differences between the resistant and susceptible varieties (Figure 5B, Wilcoxon test, p-value >0.005).

3.7 | Taxonomic Structure and Relative Abundance of the Dominant Microbial Communities

We identified 18 bacterial and four fungal phyla within the rapeseed microbiome. Proteobacteria were the most prevalent bacterial phylum in both resistant and susceptible samples, with a relative abundance ranging from 52% in susceptible and 58% in resistant varieties (Figure 6A, Table S2). The second most prevalent phylum was *Actinobacteria*, constituting 21% of the relative abundance in both varieties. *Firmicutes* represented approximately 13% of the bacterial community

TABLE 3 | MTAs linked to Sclerotinia stem rot (SSR) resistance in oilseed rape accessions.

SNP	Allele	Chr	Pos	p	MAF	Effect	Model
Relative lesion area (RLA)							
Bn-A01-p19174115	G/A	A01	19,174,115	0.00058	0.46	-0	Blink, FarmCPU
Bn-A01-p5265598	T/C	A01	5,265,598	0.00053	0.44	0.02	Blink, FarmCPU
Bn-A01-p5269368	A/G	A01	5,269,368	0.00034	0.46	-0	Blink, FarmCPU
Bn-A03-p10027020	C/A	A03	10,027,020	0.00084	0.3	-0	Blink, FarmCPU
Bn-A06-p1015217	A/G	A06	1,015,217	0.00084	0.5	-0	Blink, FarmCPU
Bn-A07-p14766907	G/T	A07	14,766,907	0.00024	0.35	-0	Blink, FarmCPU
Bn-A07-p14768265	C/T	A07	14,768,265	0.00024	0.35	-0	Blink, FarmCPU
Bn-A07-p14770619	C/A	A07	14,770,619	0.00043	0.34	0.02	Blink, FarmCPU
Bn-A07-p14792267	C/A	A07	14,792,267	0.00016	0.36	0.02	Blink, FarmCPU
Bn-A07-p15165145	C/T	A07	15,165,145	0.00026	0.35	-0	Blink, FarmCPU
Bn-A07-p17388825	C/T	A07	17,388,825	0.00092	0.09	-0	Blink, FarmCPU
Lesion area (LA)							
Bn-A01-p2291940	C/T	A01	2,291,940	0.00016	0.48	-0.8	Blink, FarmCPU
Bn-A01-p24575577	T/C	A01	24,575,577	6.58E-05	0.12	-1	Blink, FarmCPU
Bn-A01-p4353657	T/C	A01	4,353,657	0.00024	0.35	0.97	Blink, FarmCPU
Bn-A02-p23835683	C/A	A02	23,835,683	0.00082	0.42	-0.8	Blink, FarmCPU
Bn-A03-p12541207	A/G	A03	12,541,207	0.00049	0.11	0.96	Blink, FarmCPU
Bn-A04-p4848743	C/T	A04	4,848,743	0.00059	0.4	0.74	Blink, FarmCPU
Bn-A04-p4932716	C/T	A04	4,932,716	0.00019	0.29	0.79	Blink, FarmCPU
Bn-A04-p5137321	C/T	A04	5,137,321	0.00089	0.34	0.69	Blink, FarmCPU
Bn-A06-p6023926	T/C	A06	6,023,926	0.00043	0.46	0.85	Blink, FarmCPU
Bn-scaff_16534_1-p679107	G/A	C04	3,245,237	9.86E-05	0.48	-1.3	Blink, FarmCPU
Bn-scaff_16534_1-p692624	C/T	C04	3,268,224	0.00042	0.48	1.16	Blink, FarmCPU
Bn-scaff_16534_1-p707801	C/T	C04	3,285,208	7.9E-05	0.47	1.29	Blink, FarmCPU
Bn-scaff_16876_1-p712918	A/G	C04	34,199,365	0.00091	0.24	0.65	Blink, FarmCPU
Bn-scaff_17109_4-p283045	G/A	C02	40,663,064	0.00072	0.3	-0.8	Blink, FarmCPU
Bn-scaff_17972_1-p401085	A/G	C07	31,133,080	0.00051	0.25	-1	Blink, FarmCPU
Bn-scaff_17972_1-p424888	T/C	C07	31,111,744	0.00036	0.24	1.05	Blink, FarmCPU
Bn-scaff_17972_1-p425274	C/A	C07	31,111,358	0.00012	0.27	1.11	Blink, FarmCPU
Bn-scaff_17972_1-p425760	A/C	C07	31,110,872	0.00045	0.26	-1	Blink, FarmCPU
Bn-scaff_17972_1-p486112	G/A	C07	486,112	0.00083	0.26	0.95	Blink, FarmCPU
Bn-scaff_17972_1-p570410	C/T	C07	31,007,851	0.00097	0.24	-0.9	Blink, FarmCPU
Bn-scaff_18360_1-p35474	A/C	C02	35,867,356	0.00044	0.33	0.83	Blink, FarmCPU
Bn-scaff_18936_1-p1066008	A/C	C03	3,604,701	0.00039	0.46	-1	Blink, FarmCPU
Bn-scaff_22067_1-p209140	T/G	C03	20,809,524	6.79E-06	0.3	-0.9	Blink, FarmCPU
Bn-scaff_22451_2-p224920	T/G	C02	25,698,199	0.00085	0.47	0.97	Blink, FarmCPU
Bn-scaff_22451_2-p258637	A/G	C02	25,724,340	0.0006	0.47	-1	Blink, FarmCPU

(Continues)

SNP	Allele	Chr	Pos	р	MAF	Effect	Model
Bn-scaff_22451_2-p77323	C/A	C02	77,323	0.00029	0.46	1.09	Blink, FarmCPU
Lesion length (LL)							
Bn-A04-p10555408	C/A	A04	10,555,408	0.00044	0.39	0.69	Blink, FarmCPU
Bn-A07-p12487549	G/A	A07	12,487,549	0.00091	0.4	-0.7	Blink, FarmCPU
Bn-A09-p4652268	T/G	A09	4,652,268	0.00094	0.26	0.81	Blink, FarmCPU
Bn-A09-p4916858	C/A	A09	4,916,858	0.00087	0.24	0.86	Blink, FarmCPU
Bn-scaff_16197_1-p2487005	C/T	C08	31,723,896	0.00074	0.36	-0.8	Blink, FarmCPU
Bn-scaff_16394_1-p1516390	T/C	C04	32,954,774	0.00029	0.18	-1.4	Blink, FarmCPU
Bn-scaff_16414_1-p175360	G/A	C05	1,654,223	0.00028	0.39	-0.8	Blink, FarmCPU
Bn-scaff_16445_1-p1548555	T/C	C08	35,214,192	0.00066	0.31	0.83	Blink, FarmCPU
Bn-scaff_21925_1-p107332	C/T	C04	1,741,974	0.00056	0.43	0.65	Blink, FarmCPU
Bn-scaff_22970_1-p213807	C/T	C02	213,807	0.00037	0.38	0.94	Blink, FarmCPU

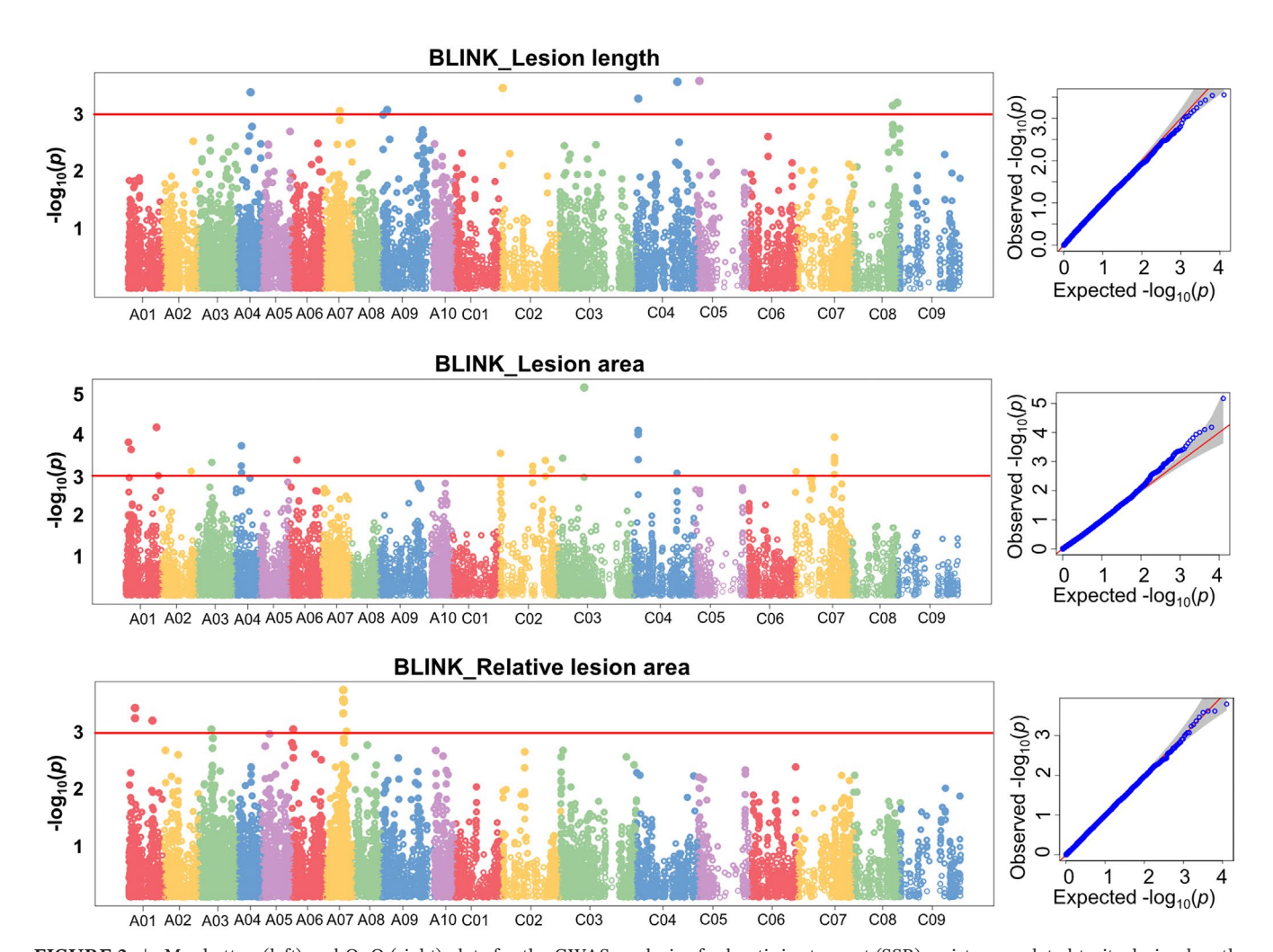


FIGURE 3 | Manhattan (left) and Q-Q (right) plots for the GWAS analysis of sclerotinia stem rot (SSR) resistance-related traits: lesion length, lesion area, and relative lesion area in oilseed rape accessions.

(Table S2). Additionally, *Bacteroidota* contributed to approximately 5%–6% of the total relative abundance (Figure 6A). In the fungal community, the phylum *Ascomycota* was the

most abundant in resistant and susceptible samples, with relative abundances ranging from 58% to 64% (Figure 6B and Table S3). This was followed by *fungi-phy-incertae sedis*,

25756265, 2025, 5, Downloaded from https://onlinelibrary.wiley.com/doi/10.1002/pei3.70092 by Swedish University Of Agricultural Sciences, Wiley Online Library on [13/11/2025]. See the Terms

nditions) on Wiley Online Library for rules of use; OA articles are governed by the applicable Creative Commons Licens

Plant-Environment Interactions, 2025 9 of 18

TABLE 4 | MTAs linked to chlorophyll content and stability in oilseed rape accessions.

SNP	Allele	Chr	Pos	р	MAF	Effect	Model
Chlorophyll index (CI)							
Bn-A02-p26154951	A/G	A02	26,154,951	0.00049	0.17	-1.79	FarmCPU
Bn-A04-p11329756	T/G	A04	11,329,756	1.46E-06	0.26	1.82	Blink
Bn-A05-p967131	C/T	A05	967,131	2.74E-07	0.1	-2.11	Blink
Bn-scaff_20461_1-p249973	A/G	C02	9,420,451	5.73E-11	0.48	-2.39	Blink, FarmCPU
Bn-scaff_20461_1-p178421	T/C	C02	178,421	0.00017	0.43	1.94	FarmCPU
Bn-scaff_20461_1-p99520	A/G	C02	9,562,691	0.00027	0.49	-2.06	FarmCPU
Bn-scaff_20461_1-p110039	G/A	C02	9,550,142	0.00056	0.46	1.83	FarmCPU
Bn-scaff_15832_1-p52737	C/A	C04	378,587	5.12E-08	0.37	-1.41	Blink
Bn-scaff_16361_1-p1343410	A/G	C08	28,813,035	0.0003	0.48	1.52	FarmCPU
Bn-scaff_16361_1-p935272	G/A	C08	28,413,763	0.00036	0.43	1.5	FarmCPU
Bn-scaff_16197_1-p659483	T/C	C08	33,364,657	0.00038	0.26	-0.99	Blink
SPAD healthy (SPADH)							
Bn-A02-p27203061	G/A	A02	27,203,061	0.00046	0.49	0.51	Blink, FarmCPU
Bn-A03-p14583041	T/G	A03	14,583,041	0.00052	0.48	-0.61	Blink, FarmCPU
Bn-A05-p20141883	T/G	A05	20,141,883	0.00086	0.4	-0.59	Blink, FarmCPU
Bn-A06-p6439396	G/A	A06	6,439,396	0.00018	0.26	0.87	Blink, FarmCPU
Bn-A06-p1768254	G/A	A06	1,768,254	0.0002	0.4	0.6	Blink, FarmCPU
Bn-A10-p2268881	G/A	A10	2,268,881	0.00056	0.26	0.79	Blink, FarmCPU
Bn-scaff_15818_2-p1213540	A/G	C06	17,603,819	0.00099	0.18	-0.67	Blink, FarmCPU
SPAD infected (SPADI)							
Bn-A08-p16859028	A/G	A08	16,859,028	0.00013	0.36	0.89	Blink, FarmCPU
Bn-scaff_20461_1-p249973	A/G	C02	9,420,451	7.71E-05	0.48	-1.16	Blink, FarmCPU
Bn-scaff_20461_1-p178421	T/C	C02	178,421	0.00018	0.43	1.08	Blink, FarmCPU
Bn-scaff_15712_5-p313157	A/G	C02	313,157	0.00074	0.42	-1.178	Blink, FarmCPU
Bn-scaff_20942_1-p1093417	C/T	C02	1,093,417	0.00087	0.45	-1.15	Blink, FarmCPU
Bn-scaff_16361_1-p1343410	A/G	C08	28,813,035	0.00054	0.48	0.82	Blink, FarmCPU

constituting 31%–33% of the fungal community (Table S3). The phylum *Basidiomycota* contributed 4%–7% to the resistant and susceptible samples (Figure 6B).

The most abundant bacterial genera were *Pseudomonas*, *Methylobacterium*, *Sphingomonas*, *Staphylococcus*, *Microbacterium*, and *Aquabacterium* (Figure 6C). Genera such as *Pseudomonas*, *Methylobacterium*, *Aquabacterium*, *Yersinia*, and *Cutibacterium* were more prevalent in resistant samples (Figure 6C, Table S4). In contrast, *Sphingomonas*, *Staphylococcus*, and *Microbacterium* were more abundant in susceptible samples (Figure 6C). Moreover, the linear discriminant analysis (LDA) revealed the specific taxa responsible for the observed significant differences in the composition of resistant and susceptible microbiomes (Figure 7A). Five taxa were

significantly enriched in resistant varieties and had an LDA score of > 4. The most enriched taxa were *Pseudomonas* (genus), *Pseudomonadales* (Order), *Pseudomonadaceae* (Family), and *Pseudomonas* (Species). Nine taxa significantly differed in susceptible oilseed varieties. The members of the *Micrococcales* (order) had a larger size effect with an LDA score > 4, followed by *Sphingobactriales* and *Massilia* (Figure 7A).

The three most abundant genera across all samples for the fungal community were *Penicillium*, *Cladosporium*, and genera classified as *fungi_gen_ Incertae_sedis* (Figure 6D, Table S5). Although the relative abundance of these fungal genera remained relatively stable between resistant and susceptible samples, LDA showed that resistant varieties had nine enriched taxa. In comparison, susceptible varieties had only one (*Cystobasidium*

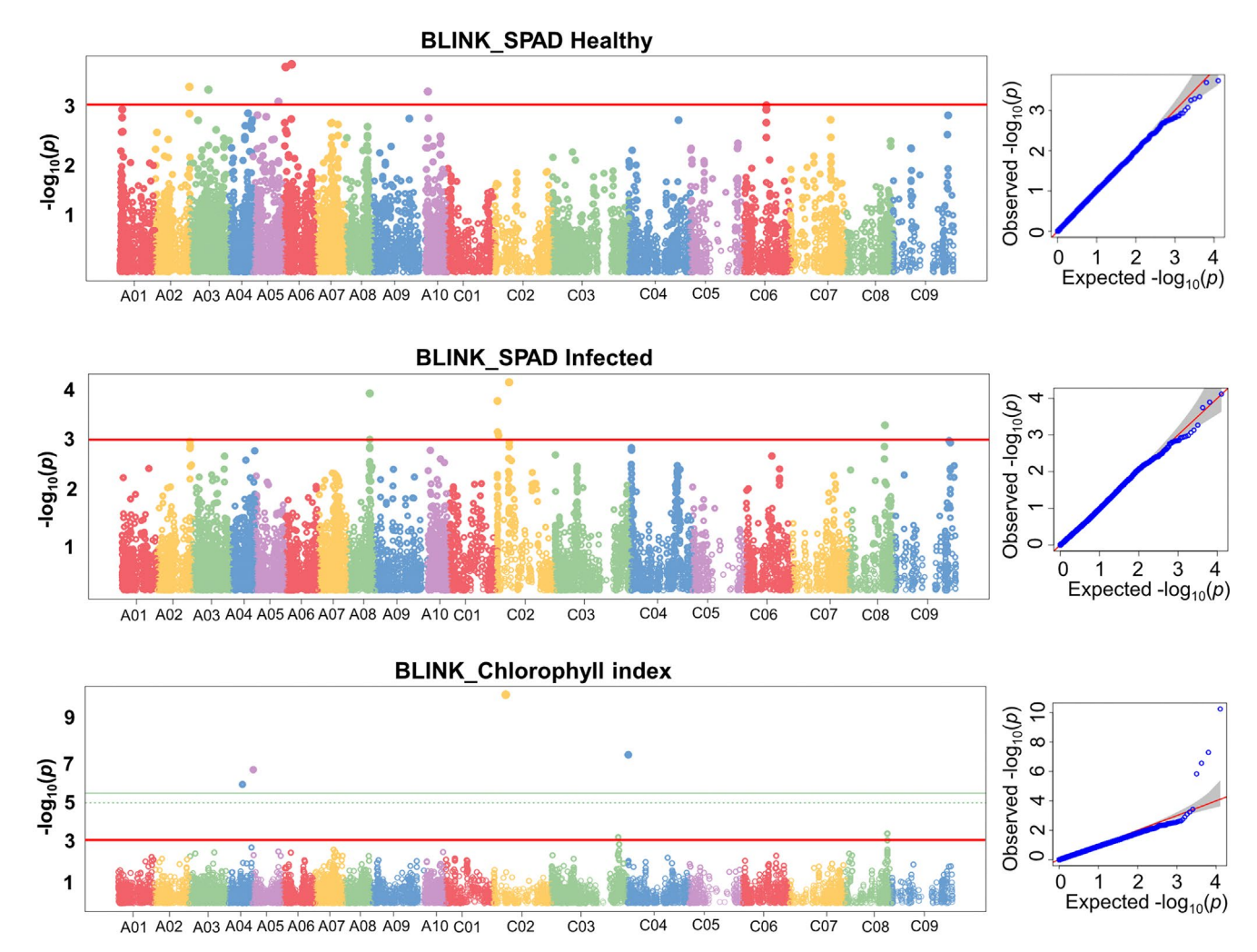


FIGURE 4 | Manhattan (left) and Q–Q (right) plots for the GWAS for the SPAD measurements in healthy leaves before inoculation (SPADH), at 3 days post inoculation (SPADI) with Sclerotinia stem rot (SSR), and the chlorophyll index (CI) in oilseed rape accessions.

_laryngis) differentially enriched taxon (Figure 7B). The most enriched taxa in resistant varieties were members of the Mycosphaerellales, Thelebolales, and Akanthomyces (Figure 7B).

3.8 | SSR-Related Variants Contributing to SSR Resistance and Microbial Recruitment

The most relatively susceptible and resistant accessions of the oilseed rape germplasm were used for investigating the microbiome recruitment variation between these groups. The resistant group had relatively lower lesion length (LL), lesion area (LA), and relative lesion area (RLA) compared to the susceptible group (Figure S1A). However, there was no significant difference between the resistant and susceptible groups for the SPADH, SPADI, and CI values (Figure S1B). The allelic variations in the 47 MTAs detected linked to SSR resistance (Table 5) between these resistance and susceptible groups are presented (Table S6). The most consistent allele variation between resistance and susceptible groups was MTAs associated with the lesion length. The top four MTAs with the most significant phenotypic effect were Bn-A09-p4652268 (T/G) and Bn-A09-p4916858 (C/A) located on A09, and Bn-scaff_22970_1-p213807 (C/T) and Bn-scaff_16414_1-p175360 (G/A) located on C02 and C05 respectively (Table 5). In the whole oilseed rape germplasm investigated, the mean lesion length value for the favorable allele, found commonly in resistant accessions, was smaller compared to the alternative allele commonly found in the susceptible group (Figure 8).

4 | Discussion

Identifying resistance genotypes within a diverse germplasm and detecting the genetic basis for resistance is critical for enhancing host resistance and developing resistant varieties of economically important crops. This is particularly important to mitigate the impact of Sclerotinia stem rot on oilseed rape production, as cultural control practices are ineffective and laborious, and it is difficult to predict the optimal time for applying fungicides (Derbyshire and Denton-Giles 2016). However, there is no oilseed rape genotype with complete resistance against the pathogen that has been found so far (Neik et al. 2017; Ding et al. 2021). Given the population structure and aggressiveness, as well as the rich effector repertoire diversity of the pathogen (Taylor et al. 2015; Yu et al. 2020; Gupta et al. 2022), as well as resistance variation among subpopulations of oilseed rape (Neik et al. 2017), investigating the resistance in locally adapted germplasm would provide resistance sources for

Plant-Environment Interactions, 2025

S Ξ 7 \geq Susceptible S \ge ⋖ S \geq Z ~ 2 c ⋈ ~ ~ \geq Z Resistant \simeq Z ~ ⋖ ~ Z 10,555,408 2,487,549 4,652,268 4,916,858 1,741,974 Pos (bp) 213,807 C04 A07 A09 Alleles Bn-scaff_22970_1-p213807 Bn-scaff_21925_1-p107332 Bn-A07-p12487549 Bn-A04-p10555408 Bn-A09-p4652268 Bn-A09-p4916858 Marker

c

b

c

c

1,654,223

C05

G/A

Bn-scaff_16414_1-p175360

breeding programs targeted at particular regions. Enhancing the level of resistance in oilseed rape through the pyramiding of existing partial resistance is challenging because the QTLs for such resistance explain only a low percentage of the phenotypic variations and lack reproducibility (Ding et al. 2021). Hence, beyond the genetics approach, understanding agronomic and physiological processes contributing to enhanced levels of the existing partial resistance in oilseed rape is needed to limit the impact of the disease.

4.1 | Sclerotinia Stem Rot Resistance in Oilseed Rape Accessions

In total, 47 MTAs spanning across all chromosomes except A10, C01, and C06 were detected, associated with the SSR resistance traits LL, LA, and RLA. Twenty-four of these MTAs were from the A-subgenome and 26 from the C-subgenome of the crop, with chromosomes A07 and C07 contributing seven and six MTAs. This is in agreement with previous findings, which showed that SSR resistance is a complex trait controlled by several QTLs with minor effects (Wei et al. 2014; Wu et al. 2016; Roy et al. 2021). The findings indicate that both subgenomes play a crucial role in the SSR resistance of oilseed rape. A different set of significant SNPs was identified for Stem lesion length and Stem lesion width (Roy et al. 2021, 2024), and 17 SNPs for stem lesion length (Wei et al. 2016) have been previously identified in oilseed rape. These studies were based on field experiments and stem tissue, but the results suggest the possibility of finding different SNPs for SSR resistance traits LL, LA, and RLA found in the current study. Analyzing several aspects of the Sclerotinia stem rot disease growth on plant tissue is crucial for establishing a relationship between the disease symptoms and the genetic bases regulating genotype-specific resistance response to the pathogen. However, the MTAs detected in this study had a minimal effect on the phenotypes measured compared to the previous studies (Wei et al. 2016; Roy et al. 2021, 2024). This could be due to the less number of accessions investigated in the present study, and the previous studies were focused on stem resistance, conducted in field conditions; hence, microclimate factors can influence SSR disease development and plant response (Ficke et al. 2018). However, all the significant SNPs associated with SSR resistance were detected using the most stringent models, Blink (Huang et al. 2018) and FarmCPU models (Liu et al. 2016), which show the relevance of the MTAs under the current study conditions. Indeed, we found SNPs consistently differ between the relatively resistant and susceptible groups, with the favorable alleles showing lower LL, LA, and RLA compared to the alternative alleles. Particularly, the SNPs linked to LL Bn-A09-p4652268, Bn-A09-p4916858, Bn-scaff_22970_1-p213807, Bn-scaff 16414 1-p175360 were interesting as the alleles segregate in the most relatively resistant and susceptible accessions used for the microbial recruitment investigation.

4.2 | Chlorophyll Level During the Sclerotinia Stem Rot Infection

SSR infection reduces the leaf area for photosynthesis; hence, maintaining high chlorophyll content is crucial for producing photosynthate and reducing yield loss due to the pathogen infection. A total of seven MTAs were detected for SPADH, six MTAs for SPADI, and 11 MTAs for CI. Of these MTAs, Bn-scaff_20461_1-p249973

Allele variation between the most resistant (R) and susceptible (S) oilseed rape accessions.

FABLE 5

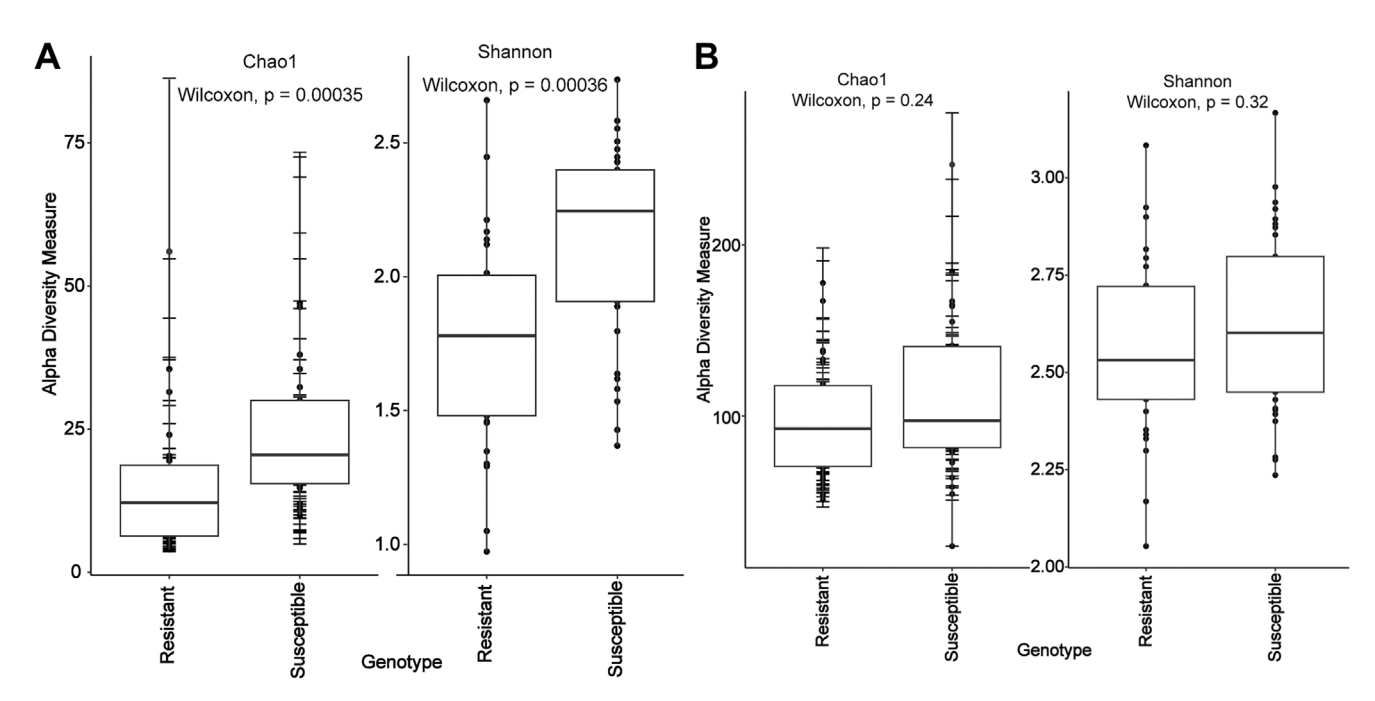


FIGURE 5 | Microbial community analysis: Bacterial (A) and fungal (B) communities' alpha diversity measures in resistant and susceptible rapeseed varieties using Chao1 and Shannon indexes. Statistical significance was determined using the Wilcoxon test.

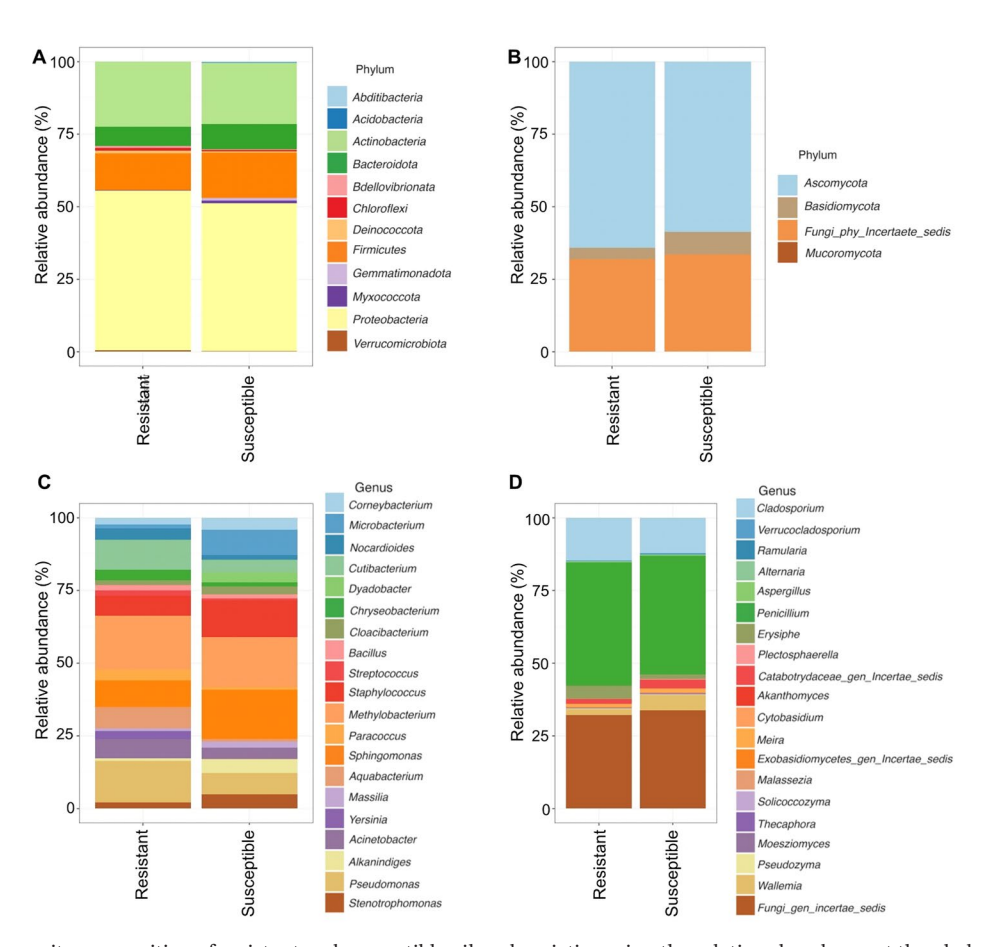


FIGURE 6 | Community composition of resistant and susceptible oilseed varieties using the relative abundance at the phylum and genus levels. The relative abundance of the most abundant phyla in bacteria (A) and fungi (B), followed by the relative abundance of the top 20 bacterial (C) and fungal (D) genera, was visualized in the bar chart.

Plant-Environment Interactions, 2025

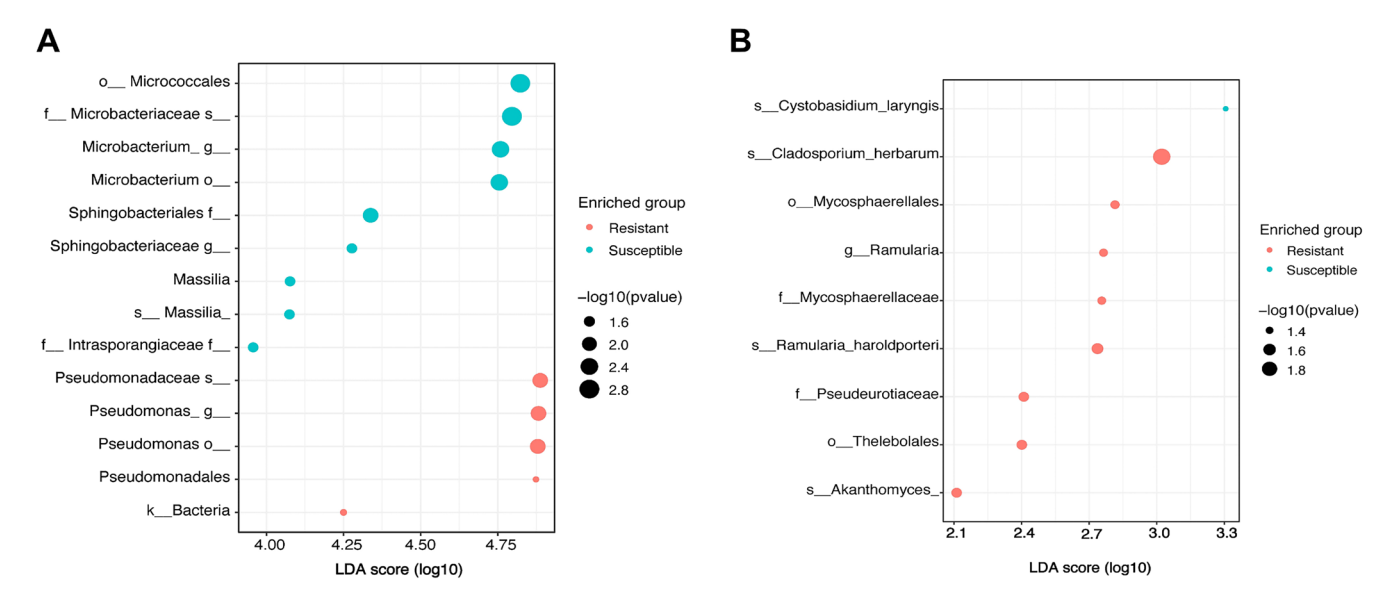


FIGURE 7 | Differential abundance analysis using linear discriminant analysis (LDA). This figure shows the differentially abundant bacterial taxa (A) and fungal taxa (B) identified in resistant and susceptible oilseed rape accessions.

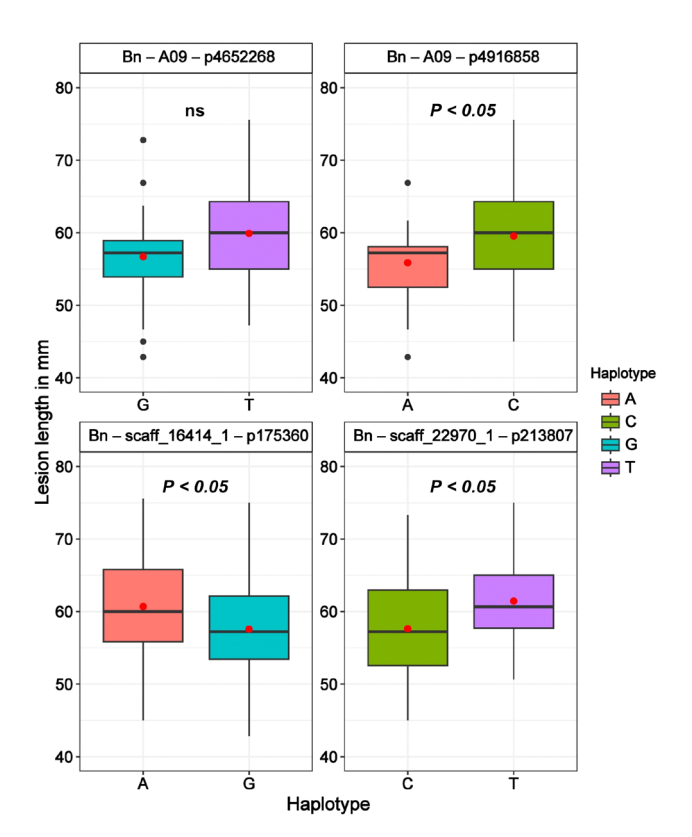


FIGURE 8 | Contribution of the favorable and alternative alleles of the MTAs for the lesion length variation among the oilseed rape accessions.

and Bn-scaff_20461_1-p178421, located on C02, and Bn-scaff_16361_1-p1343410, located on C08, were associated with SPADI and CI. CI is an important trait because the SSR is a necrotrophic fungus (Gupta et al. 2022) that reduces the leaf area; hence, the SPADI. Considering this, CI is an important trait in maintaining the chlorophyll levels and the photosynthetic rate. Chlorophyll indices could be used for detecting plant diseases (Odilbekov

et al. 2018; Koc et al. 2022). In agreement with this study, a significant majority of the 281 single-nucleotide polymorphisms (SNPs) associated with photosynthetic pigment (Xu et al. 2022) and 10 out of 14 SNPs linked to chlorophyll synthesis (Hu et al. 2022) in oilseed rape were located in the C-subgenome. Moreover, a chlorophyll-deficient dominant locus (CDE1) in oilseed rape was mapped to C08 (Wang et al. 2016). The findings indicate the C-subgenome's crucial role in maintaining the chlorophyll content and photosynthesis rate, and both traits should be considered as SSR resistance-related traits in oilseed rape.

4.3 | Microbial Recruitment in Sclerotinia-Resistant and Susceptible Oilseed Rape Accessions

The composition and structure of the phyllosphere are critical to its impact on the host plant, highlighting the need to understand the mechanisms behind its assembly and dynamics (Hawkes et al. 2021). Plant genotype is a crucial factor influencing the microbial diversity of the phyllosphere. Our study investigates the microbiota of resistant and susceptible oilseed rape varieties, focusing on bacterial and fungal communities. We found significant differences in bacterial diversity between the two genotypes, while fungal communities remained unaffected by these variations.

The genetic variations between resistant and susceptible oil-seed rape varieties notably influence bacterial diversity. The observed higher alpha diversity in the susceptible oilseed rape varieties than in resistant ones could be due to several factors. For instance, susceptible varieties are more prone to pathogen infection, leading to severe tissue damage and a weaker immune system. This environment allows a broader range of microbes to coexist, including opportunistic pathogens and commensals. Moreover, the compromised defense mechanism in susceptible plants leads to frequent invasions by environmental microbes, contributing to higher microbial diversity. Conversely, the

14 of 18 Plant-Environment Interactions, 2025

robust immune system in the resistant varieties suppresses the invasion of certain microbes, selectively enriching the specific microbial communities and resulting in less diverse but specialized microbial communities.

In this study, this selective enrichment is more evident by the significantly enriched members of the *Pseudomonas* in resistant oilseed rape varieties. Genus *Pseudomonas* is widely known for its role in plant growth promotion and biological control of plant diseases. These bacteria are ubiquitous in nature and are characterized by their versatile metabolic activities. Strains and species of this genus enhance plant growth by facilitating nutrient acquisition, regulating plant hormone levels, and inducing a systemic response in plants through disease suppression (biological control). They achieve this via the production of antibiotics and the regulation of signaling molecules (Kumar et al. 2017; Jegan et al. 2018). Additionally, resistant varieties enriched the phyllosphereabundant genus *Methylobacterium*, which is known to promote plant growth and development (Dourado et al. 2015).

Moreover, fungal communities significantly enriched in resistant varieties such as Thelebolales and Pseuderotiaceae are known to produce secondary metabolites, antifreeze proteins, and ice-freezing proteins, which strengthen the resistance of the oilseed rape microbiome. Besides, the species *Akanthomyces* ensures protection against a wide array of pests, including antifungal and bacterial activity against *Sclerotinia sclerotiorum*, *Rhizoctonia solani*, *Aspergillus flavus*, and *Staphylococcus aureus* pathogens (Gurulingappa et al. 2010; Dash et al. 2018; Nicoletti and Becchimanzi 2020).

On the other hand, susceptible oilseed rape varieties exhibited higher abundances of genera associated with stress tolerance (Sphingomonas) (Asaf et al. 2020) and plant growth and disease control (Stenotrophomonas and Microbacterium) (Kumar et al. 2023). Bacterial species from the genera Microbacterium and Stenotrophomonas were identified at blast lesion, which reduced the blast severity and promoted plant growth (Behrendt et al. 2001; Md Gulzar and Mazumder 2023). These findings suggest that an increased abundance of specific microbial taxa in different genotypes could recruit specific ones to fulfill their demands. This implies that genetic differences in oilseed rape varieties may drive selective enrichment of certain bacterial taxa's relative abundance and recruit specific microbes rather than exclude them. Mainly, phyla Proteobacteria and Bacteroidota were the most responsive to these genotype variations, similar to previous reports (Taye et al. 2020).

Unlike bacterial communities, fungal communities exhibited stable diversity despite minor changes in the relative abundance of dominant taxa. This stability indicates that fungal assemblages are less influenced by the host plant's genetic variations and more affected by factors such as geographical location and environmental stress (Barret et al. 2015, 2016). This stable fungal community structure across resistant and susceptible varieties suggests that the phyllosphere fungal composition does not directly influence the resistance function observed in these oil-seed rape varieties.

Overall, this study highlights the impact of genetic variation on the dynamics of the phyllosphere microbial community. The higher relative dominance of specific microbial taxa supports the notion that plants actively select particular microbial communities to meet their requirements. These findings imply that breeding for specific resistance traits in oilseed rape could indirectly influence the composition and function of the phyllosphere microbiome. These findings contribute to a better understanding of the relationships between plant genotypes and their associated microbiomes, with potential implications for agricultural practices and crop improvement strategies.

5 | Conclusion

The study provided the genetic regions playing a crucial role in Sclerotinia stem rot resistance and maintaining the chlorophyll content during the infection. As the pathogen expands on the leaf and the photosynthetic efficient area reduces, hence increasing or maintaining higher chlorophyll content on the uninfected part of the leaf could be a tolerance mechanism in oilseed rape for reducing the impact of the pathogen on yield and quality. Importantly, the SSR resistance level and chlorophyll index differences between the resistant and susceptible accessions were reflected in the microbial composition. The study has limitations related to the size of the GWAS panel, and only one strain of Sclerotinia was used for resistance screening. However, the study provides insights into multifaceted strategies and their genetic basis for applying breeding techniques to improve the resistance and further enhance the resistance level by taking into consideration the genetic basis of the resistance phenotype, chlorophyll index, and microbial recruitment in oilseed rape.

Acknowledgments

K.B.A. acknowledges support from KSLA (GFS2021-0082).

Conflicts of Interest

The authors declare no conflicts of interest.

Data Availability Statement

All data generated and analyzed in this study are included in the submitted manuscript. All of the amplicon data (16S&ITS) were submitted to the sequence read archive repository under BioProject: Id PRJNA1063738. Genotype data for the rapeseed accessions is available in the Figshare repository: https://figshare.com/s/5c84342043939c2 a34a5 (Doi: https://doi.org/10.6084/m9.figshare.28665032).

References

Alvarado, G., F. M. Rodríguez, A. Pacheco, et al. 2020. "META-R: A Software to Analyze Data From Multi-Environment Plant Breeding Trials." *Crop Journal* 8, no. 5: 745–756. https://doi.org/10.1016/j.cj.2020. 03.010.

Asaf, S., M. Numan, A. L. Khan, and A. Al-Harrasi. 2020. "Sphingomonas: From Diversity and Genomics to Functional Role in Environmental Remediation and Plant Growth." *Critical Reviews in Biotechnology* 40, no. 2: 138–152.

Barret, M., M. Briand, S. Bonneau, et al. 2015. "Emergence Shapes the Structure of the Seed Microbiota." *Applied and Environmental Microbiology* 81, no. 4: 1257–1266.

Plant-Environment Interactions, 2025

- Barret, M., J. F. Guimbaud, A. Darrasse, and M. A. Jacques. 2016. "Plant Microbiota Affects Seed Transmission of Phytopathogenic Microorganisms." *Molecular Plant Pathology* 17, no. 6: 791–795.
- Behrendt, U., A. Ulrich, and P. Schumann. 2001. "Description of *Microbacterium foliorum* sp. Nov. and *Microbacterium phyllosphaerae* sp. Nov., Isolated From the Phyllosphere of Grasses and the Surface Litter After Mulching the Sward, and Reclassification of *Aureobacterium resistens* (Funke Et al. 1998) as *Microbacterium resistens* Comb. Nov." *International Journal of Systematic and Evolutionary Microbiology* 51, no. 4: 1267–1276.
- Bolyen, E., J. R. Rideout, M. R. Dillon, et al. 2019. "Reproducible, Interactive, Scalable and Extensible Microbiome Data Science Using QIIME 2." *Nature Biotechnology* 37, no. 8: 852–857. https://doi.org/10.1038/s41587-019-0209-9.
- Bradbury, P. J., Z. Zhang, D. E. Kroon, T. M. Casstevens, Y. Ramdoss, and E. S. Buckler. 2007. "TASSEL: Software for Association Mapping of Complex Traits in Diverse Samples." *Bioinformatics* 23, no. 19: 2633–2635. https://doi.org/10.1093/bioinformatics/btm308.
- Callahan, B. J., P. J. McMurdie, M. J. Rosen, A. W. Han, A. J. Johnson, and S. P. Holmes. 2016. "DADA2: High-Resolution Sample Inference From Illumina Amplicon Data." *Nature Methods* 13, no. 7: 581–583. https://doi.org/10.1038/nmeth.3869.
- Cao, Y., Q. Dong, D. Wang, P. Zhang, Y. Liu, and C. Niu. 2022. "microbiomeMarker: An R/Bioconductor Package for Microbiome Marker Identification and Visualization." *Bioinformatics* 38, no. 16: 4027–4029. https://doi.org/10.1093/bioinformatics/btac438.
- Chew, S. C. 2020. "Cold-Pressed Rapeseed (*Brassica napus*) Oil: Chemistry and Functionality." *Food Research International* 131: 108997. https://doi.org/10.1016/j.foodres.2020.108997.
- Dahanayaka, B. A., and A. Martin. 2023. "Multi-Parental Fungal Mapping Population Study to Detect Genomic Regions Associated With *Pyrenophora teres* f. *teres* Virulence." *Scientific Reports* 13, no. 1: 9804. https://doi.org/10.1038/s41598-023-36963-y.
- Dash, C. K., B. S. Bamisile, R. Keppanan, et al. 2018. "Endophytic Entomopathogenic Fungi Enhance the Growth of *Phaseolus vulgaris* L. (Fabaceae) and Negatively Affect the Development and Reproduction of *Tetranychus urticae* Koch (Acari: Tetranychidae)." *Microbial Pathogenesis* 125: 385–392.
- Derbyshire, M. C., and M. Denton-Giles. 2016. "The Control of Sclerotinia Stem Rot on Oilseed Rape (*Brassica napus*): Current Practices and Future Opportunities." *Plant Pathology* 65, no. 6: 859–877. https://doi.org/10.1111/ppa.12517.
- Ding, L. N., T. Li, X. J. Guo, et al. 2021. "Sclerotinia Stem Rot Resistance in Rapeseed: Recent Progress and Future Prospects." *Journal of Agricultural and Food Chemistry* 69, no. 10: 2965–2978. https://doi.org/10.1021/acs.jafc.0c07351.
- Dixon, P. 2003. "VEGAN, a Package of R Functions for Community Ecology." *Journal of Vegetation Science* 14: 927–930.
- Dourado, M. N., A. Aparecida Camargo Neves, D. S. Santos, and W. L. Araújo. 2015. "Biotechnological and Agronomic Potential of Endophytic Pink-Pigmented Methylotrophic *Methylobacterium* spp." *BioMed Research International* 2015, no. 1: 909016.
- FAOSTAT. 2023. "Food and Agriculture Organization of the United Nations." Accessed March 31, 2024. http://www.fao.org/faostat/en/.
- Feng, Y. X., Y. X. Hu, P. P. Fang, et al. 2021. "Silicon Alleviates the Disease Severity of Sclerotinia Stem Rot in Rapeseed." *Frontiers in Plant Science* 12: 721436. https://doi.org/10.3389/fpls.2021.721436.
- Ficke, A., C. Grieu, M. B. Brurberg, and G. Brodal. 2018. "The Role of Precipitation, and Petal and Leaf Infections in Sclerotinia Stem Rot of Spring Oilseed Brassica Crops in Norway." *European Journal of Plant Pathology* 152, no. 4: 885–900. https://doi.org/10.1007/s10658-018-1569-6.

- Gupta, N. C., S. Yadav, S. Arora, et al. 2022. "Draft Genome Sequencing and Secretome Profiling of *Sclerotinia sclerotiorum* Revealed Effector Repertoire Diversity and Allied Broad-Host Range Necrotrophy." *Scientific Reports* 12, no. 1: 21855. https://doi.org/10.1038/s41598-022-22028-z.
- Gurulingappa, P., G. A. Sword, G. Murdoch, and P. A. McGee. 2010. "Colonization of Crop Plants by Fungal Entomopathogens and Their Effects on Two Insect Pests When In Planta." *Biological Control* 55, no. 1: 34–41.
- Hawkes, C. V., R. Kjøller, J. M. Raaijmakers, et al. 2021. "Extension of Plant Phenotypes by the Foliar Microbiome." *Annual Review of Plant Biology* 72: 823–846.
- Hu, J. H., B. Y. Chen, J. Zhao, et al. 2022. "Genomic Selection and Genetic Architecture of Agronomic Traits During Modern Rapeseed Breeding." *Nature Genetics* 54, no. 5: 694–704. https://doi.org/10.1038/s41588-022-01055-6.
- Huang, M., X. Liu, Y. Zhou, R. M. Summers, and Z. Zhang. 2018. "BLINK: A Package for the Next Level of Genome-Wide Association Studies With Both Individuals and Markers in the Millions." *GigaScience* 8, no. 2: giy154. https://doi.org/10.1093/gigascience/giy154.
- Jegan, S., R. Kathiravan, D. Purushothaman, and P. Vaiyapuri. 2018. "Potential of Finger Millet Indigenous Rhizobacterium *Pseudomonas* sp. MSSRFD41 in Blast Disease Management-Growth Promotion and Compatibility With the Resident Rhizomicrobiome." *Frontiers in Microbiology* 9: 1029.
- Koc, A., F. Odilbekov, M. Alamrani, T. Henriksson, and A. Chawade. 2022. "Predicting Yellow Rust in Wheat Breeding Trials by Proximal Phenotyping and Machine Learning." *Plant Methods* 18, no. 1: 30. https://doi.org/10.1186/s13007-022-00868-0.
- Korte, A., and A. Farlow. 2013. "The Advantages and Limitations of Trait Analysis With GWAS: A Review." *Plant Methods* 9: 29. https://doi.org/10.1186/1746-4811-9-29.
- Kumar, A., L. Rithesh, V. Kumar, et al. 2023. "Stenotrophomonas in Diversified Cropping Systems: Friend or Foe?" *Frontiers in Microbiology* 14: 1214680.
- Kumar, A., H. Verma, V. K. Singh, et al. 2017. "Role of *Pseudomonas* sp. in Sustainable Agriculture and Disease Management." In *Agriculturally Important Microbes for Sustainable Agriculture: Volume 2: Applications in Crop Production and Protection*, 195–215. Springer.
- Lahti, S. A. S. L. 2018. Microbiomeutilities: An R Package for Utilities to Guide In-Depth Marker Gene Amplicon Data Analysis. Zenodo.
- Leo Lahti, S. S. 2017. "Tools for Microbiome Analysis in R." Bioconductor.
- Liu, H. W., J. Y. Li, L. C. Carvalhais, et al. 2021. "Evidence for the Plant Recruitment of Beneficial Microbes to Suppress Soil-Borne Pathogens." *New Phytologist* 229, no. 5: 2873–2885. https://doi.org/10.1111/nph. 17057.
- Liu, S. Y., H. Raman, Y. Xiang, C. J. Zhao, J. Y. Huang, and Y. Y. Zhang. 2022. "Design of Future Rapeseed Crops: Challenges and Opportunities." *Crop Journal* 10, no. 3: 587–596. https://doi.org/10.1016/j.cj.2022.05.003.
- Liu, X., M. Huang, B. Fan, E. S. Buckler, and Z. Zhang. 2016. "Iterative Usage of Fixed and Random Effect Models for Powerful and Efficient Genome-Wide Association Studies." *PLoS Genetics* 12, no. 2: e1005767. https://doi.org/10.1371/journal.pgen.1005957.
- McMurdie, P. J., and S. Holmes. 2013. "Phyloseq: An R Package for Reproducible Interactive Analysis and Graphics of Microbiome Census Data." *PLoS One* 8, no. 4: e61217. https://doi.org/10.1371/journal.pone. 0061217.
- Md Gulzar, A., and P. Mazumder. 2023. "Plant Growth Promoting Phyllobacteria: An Effective Tool for Sustainable Agriculture." *Russian Journal of Plant Physiology* 70, no. 8: 196.

Neik, T. X., M. J. Barbetti, and J. Batley. 2017. "Current Status and Challenges in Identifying Disease Resistance Genes in *Brassica napus*." *Frontiers in Plant Science* 8: 1788. https://doi.org/10.3389/fpls.2017.

Nicoletti, R., and A. Becchimanzi. 2020. "Endophytism of *Lecanicillium* and *Akanthomyces*." *Agriculture* 10, no. 6: 205.

Nilsson, R. H., K. H. Larsson, A. F. S. Taylor, et al. 2019. "The UNITE Database for Molecular Identification of Fungi: Handling Dark Taxa and Parallel Taxonomic Classifications." *Nucleic Acids Research* 47, no. D1: D259–D264. https://doi.org/10.1093/nar/gky1022.

Odilbekov, F., R. Armoniené, T. Henriksson, and A. Chawade. 2018. "Proximal Phenotyping and Machine Learning Methods to Identify *Septoria tritici* Blotch Disease Symptoms in Wheat." *Frontiers in Plant Science* 9: 685. https://doi.org/10.3389/fpls.2018.00685.

Quast, C., E. Pruesse, P. Yilmaz, et al. 2013. "The SILVA Ribosomal RNA Gene Database Project: Improved Data Processing and Web-Based Tools." *Nucleic Acids Research* 41: D590–D596. https://doi.org/10.1093/nar/gks1219.

R Core Team. 1970. The R Stats Package: This Package Contains Functions for Statistical Calculations and Random Number Generation. R Core Team. r-project.org.

Raboanatahiry, N., H. X. Li, L. J. Yu, and M. T. Li. 2021. "Rapeseed (*Brassica napus*): Processing, Utilization, and Genetic Improvement." *Agronomy-Basel* 11, no. 9: 101794. https://doi.org/10.3390/agronomy11 091776.

Remington, D. L., J. M. Thornsberry, Y. Matsuoka, et al. 2001. "Structure of Linkage Disequilibrium and Phenotypic Associations in the Maize Genome." *Proceedings of the National Academy of Sciences of the United States of America* 98, no. 20: 11479–11484. https://doi.org/10.1073/pnas. 201394398.

Rout, K., B. G. Yadav, S. K. Yadava, et al. 2018. "QTL Landscape for Oil Content in *Brassica juncea*: Analysis in Multiple Bi-Parental Populations in High and "0" Erucic Background." *Frontiers in Plant Science* 9: 1448. https://doi.org/10.3389/fpls.2018.01448.

Roy, J., L. E. D. Mendoza, and M. Rahman. 2024. "Genome-Wide Mapping and Genomic Prediction Conditioning Sclerotinia Stem Rot Resistance in Different Ecotypes of *Brassica napus* (L.) Germplasm Collections." *Plant Stress* 11: 100395. https://doi.org/10.1016/j.stress. 2024.100395.

Roy, J., T. M. Shaikh, L. D. Mendoza, S. Hosain, V. Chapara, and M. Rahman. 2021. "Genome-Wide Association Mapping and Genomic Prediction for Adult Stage Sclerotinia Stem Rot Resistance in *Brassica napus* (L) Under Field Environments." *Scientific Reports* 11, no. 1: 21773. https://doi.org/10.1038/s41598-021-01272-9.

Rybakova, D., R. Mancinelli, M. Wikström, et al. 2017. "The Structure of the *Brassica napus* Seed Microbiome Is Cultivar-Dependent and Affects the Interactions of Symbionts and Pathogens." *Microbiome* 5: 104. https://doi.org/10.1186/s40168-017-0310-6.

Stepien, A., K. Wojtkowiak, and R. Pietrzak-Fiecko. 2017. "Nutrient Content, Fat Yield and Fatty Acid Profile of Winter Rapeseed (*Brassica napus* L.) Grown Under Different Agricultural Production Systems. *Chilean." Journal of Agricultural Research* 77, no. 3: 266–272. https://doi.org/10.4067/S0718-58392017000300266.

Tang, D. D., M. J. Chen, X. H. Huang, et al. 2023. "SRplot: A Free Online Platform for Data Visualization and Graphing." *PLoS One* 18, no. 11: e0294236. https://doi.org/10.1371/journal.pone.0294236.

Taye, Z. M., B. L. Helgason, J. K. Bell, et al. 2020. "Core and Differentially Abundant Bacterial Taxa in the Rhizosphere of Field Grown *Brassica napus* Genotypes: Implications for Canola Breeding." *Frontiers in Microbiology* 10: 3007.

Taylor, A., E. Coventry, J. E. Jones, and J. P. Clarkson. 2015. "Resistance to a Highly Aggressive Isolate of *Sclerotinia sclerotiorum* in a *Brassica*

napus Diversity Set." Plant Pathology 64, no. 4: 932–940. https://doi.org/10.1111/ppa.12327.

Team R Core. 2013. R: A Language and Environment for Statistical Computing. R Foundation for Statistical Computing. https://www.R-project.org/.

Van de Wouw, A. P., A. Idnurm, J. A. Davidson, et al. 2016. "Fungal Diseases of Canola in Australia: Identification of Trends, Threats and Potential Therapies." *Australasian Plant Pathology* 45, no. 4: 415–423. https://doi.org/10.1007/s13313-016-0428-1.

VanRaden, P. M. 2008. "Efficient Methods to Compute Genomic Predictions." *Journal of Dairy Science* 91, no. 11: 4414–4423. https://doi.org/10.3168/jds.2007-0980.

Walker, B. J., T. Abeel, T. Shea, et al. 2014. "Pilon: An Integrated Tool for Comprehensive Microbial Variant Detection and Genome Assembly Improvement." *PLoS One* 9, no. 11: e112963. https://doi.org/10.1371/journal.pone.0112963.

Wang, J., and Z. Zhang. 2021. "GAPIT Version 3: Boosting Power and Accuracy for Genomic Association and Prediction." *Genomics, Proteomics & Bioinformatics* 19, no. 4: 629–640. https://doi.org/10.1016/j.gpb.2021.08.005.

Wang, Y. K., Y. J. He, M. Yang, et al. 2016. "Fine Mapping of a Dominant Gene Conferring Chlorophyll-Deficiency in *Brassica napus*." *Scientific Reports* 6: 31419. https://doi.org/10.1038/srep31419.

Wei, D. Y., J. Q. Mei, Y. Fu, J. O. Disi, J. N. Li, and W. Qian. 2014. "Quantitative Trait Loci Analyses for Resistance to *Sclerotinia sclerotio-rum* and Flowering Time in *Brassica napus*." *Molecular Breeding* 34, no. 4: 1797–1804. https://doi.org/10.1007/s11032-014-0139-7.

Wei, L. J., H. J. Jian, K. Lu, et al. 2016. "Genome-Wide Association Analysis and Differential Expression Analysis of Resistance to Sclerotinia Stem Rot in *Brassica napus*." *Plant Biotechnology Journal* 14, no. 6: 1368–1380. https://doi.org/10.1111/pbi.12501.

Wu, J., F. Li, K. Xu, et al. 2014. "Assessing and Broadening Genetic Diversity of a Rapeseed Germplasm Collection." *Breeding Science* 64, no. 4: 321–330. https://doi.org/10.1270/jsbbs.64.321.

Wu, J., Q. Zhao, S. Liu, et al. 2016. "Genome-Wide Association Study Identifies New Loci for Resistance to Sclerotinia Stem Rot in *Brassica napus*." *Frontiers in Plant Science* 7: 1418. https://doi.org/10.3389/fpls. 2016.01418.

Xiang, Y., M. M. U. Helal, L. Liang, et al. 2023. "Genome-Wide Association Study Exposed the Pleiotropic Genes for Yield-Related and Oil Quality Traits in *Brassica napus* L." *Oil Crop Science* 8, no. 3: 156–164. https://doi.org/10.1016/j.ocsci.2023.08.001.

Xu, L. P., L. Y. Zhang, B. Yi, and Z. Q. Zhang. 2022. "Genetic Dissection of *Brassica napus* Photosynthetic Pigment Content Diversity and Identification of Loci Associated With Photoperiod and Alkaline Soil Responses." *Industrial Crops and Products* 186: 115294. https://doi.org/10.1016/j.indcrop.2022.115294.

Yu, Y., J. S. Cai, L. H. Ma, et al. 2020. "Population Structure and Aggressiveness of *Sclerotinia sclerotiorum* From Rapeseed (*Brassica napus*) in Chongqing City." *Plant Disease* 104, no. 4: 1201–1206. https://doi.org/10.1094/PDIS-07-19-1401-RE.

Zhao, C. J., M. L. Xie, L. B. Liang, et al. 2022. "Genome-Wide Association Analysis Combined With Quantitative Trait Loci Mapping and Dynamic Transcriptome Unveil the Genetic Control of Seed Oil Content in *Brassica napus* L." *Frontiers in Plant Science* 13: 929197. https://doi.org/10.3389/fpls.2022.929197.

Supporting Information

Additional supporting information can be found online in the Supporting Information section. **Figure S1:** Sclerotinia stem rot lesion length (LL), lesion area (LA) and relative lesion area (RLA) growth (A), and chlorophyll content before Sclerotinia infection (SPADH), after

infection (SPADI) and chlorophyll index (CI) values (B) in the most resistant and susceptible accessions of oil seed rape. **Table S1:** List of oilseed rape accessions used for GWAS analysis. **Table S2:** Relative abundance (%) of each bacterial amplicon sequence variant (ASV) across the resistant and susceptible rapeseed varieties at the phylum level. **Table S3:** Relative abundance (%) of each fungal amplicon sequence variant (ASV) across the resistant and susceptible rapeseed varieties at the phylum level. **Table S4:** Relative abundance (%) of each bacterial amplicon sequence variant (ASV) across the resistant and susceptible rapeseed varieties at the genus level. **Table S5:** Relative abundance (%) of each fungal amplicon sequence variant (ASV) across the resistant and susceptible rapeseed varieties at the genus level. **Table S6:** Haplotype variation, on the SNPs linked to SSR resistance, between the most resistant (R) and susceptible (S) groups of oilseed rape accessions.